Resonant Response of High-Temperature Superconducting Split-Ring Resonators

Frank Trang, *Student Member, IEEE*, Horst Rogalla, *Member, IEEE*, and Zoya Popović, *Fellow, IEEE*

***Abstract*—A study of the resonant response of high-temperature superconducting YBCO split-ring resonators (SRRs) deposited on a single crystal MgO substrate is presented. Measurement of an array of seven SRRs inside a WR-90 waveguide at temperatures below the transition temperature of YBCO ($T_c \approx 90$ K) shows a stop band centered at around 8 GHz with a 1.6-GHz bandwidth, which is also seen in the full wave simulation. An individual SRR element is measured to investigate the temperature dependence of the resonance frequency and quality factor. The single SRR measurements show a small gradual shift in the transmission resonance frequency as the temperature is lowered from 90.5 to 40 K, which can be attributed to the presence of kinetic inductance. The behavior of the measured resonance frequency versus temperature is fitted to a model to study the kinetic inductance and penetration depth. The quality factor is then calculated from the measurements in the same temperature range. Finally, the permittivity and permeability are extracted from the measured scattering parameters.**

***Index Terms*—High-temperature superconducting (HTS), MgO, split-ring resonators (SRRs), YBCO.**

I. Introduction

THE demonstration of split-ring resonators (SRRs) having a negative permeability by Pendry *et al.* [1] has led to many interesting SRR based designs and applications, including negative index materials [2]–[5], electromagnetic cloaks [6], [7], and filters [8]. SRRs have also been shown to exhibit negative permittivity [9], [10]. These experiments used normal conductors at room temperature. However, many of the demonstrated circuits exhibit significant loss, which can be reduced by using superconductors. Ricci *et al.* [11]–[13] investigated superconducting metamaterials made of Niobium (Nb) SRRs deposited on single crystal quartz substrates and Nb wires. Nb has a critical temperature (T_c) of ≈9.2 K and requires, e.g., the use of liquid Helium for cooling. Chen *et al.* [14] studied the resonant properties of terahertz high-temperature superconducting (HTS) Jerusalem cross metamaterial, made of $YBa_2Cu_3O_{7-\delta}$ (YBCO) with $\delta = 0.05$ and has a T_c of 90 K. The use of HTS in metamaterial designs is of interest since experiments can be carried out with liquid nitrogen or low cost, low power cryocoolers.

Manuscript received October 1, 2012; accepted November 24, 2012. Date of publication November 29, 2012; date of current version January 8, 2013. This work was supported by the U.S. Air Force (AFOSR) under Grant FA9550-10-1-0413.

F. Trang and Z. Popović are with the Department of Electrical, Computer, and Energy Engineering, University of Colorado, Boulder, CO 80309 USA (e-mail: frank.trang@colorado.edu).

H. Rogalla is with the Department of Electrical, Computer, and Energy Engineering, University of Colorado, Boulder, CO 80309 USA. He is also with the National Institute of Standards and Technology, Boulder, CO 80305 USA.

Color versions of one or more of the figures in this paper are available online at http://ieeexplore.ieee.org.

Digital Object Identifier 10.1109/TASC.2012.2230678

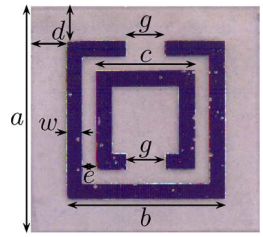

Fig. 1. Close-up photograph of the SRR unit cell with labeled dimensions, where $a = 10$ mm, $b = 7$ mm, $c = 4.4$ mm, $d = 1.5$ mm, $e = 0.5$ mm, $g = 1.6$ mm, and $w = 0.8$ mm.

In this paper, we investigate the resonant response of split-ring resonators made of YBCO film deposited on a single crystal magnesium oxide (MgO) substrate measured inside a WR-90 X-band waveguide. We will begin by briefly discussing the fabrication and geometry of the SRRs. Then, the cryogenic measurement setup, which allows for precise temperature control and the ability to study the resonances as a function of temperature, is discussed. Measurement results for multiple rings are compared to simulations. The temperature dependence of the resonance frequency and quality factor is characterized for a single SRR element. The behavior of the measured resonance frequency vs. temperature is fitted to a model to study the kinetic inductance and penetration depth. Finally, the effective permittivity and permeability are extracted from the measured scattering parameters.

II. HTS SRR Fabrication and Measurement Setup

The discovery of lanthanum barium copper oxide (LBCO) [15] superconductor quickly led to the discovery of YBCO [16], which has a T_c (≈92 K) above the boiling temperature of liquid nitrogen. Each HTS SRR unit cell in this work is made up of two 700 nm thick YBCO rings deposited on top of a 500 μm thick square slab of MgO that has a nominal relative permittivity of 9.7. The room temperature and sub-T_c electric loss tangents of MgO are 9×10^{-3} at 10 GHz [17] and 5×10^{-6} at 10.48 GHz [18], respectively. A 100 nm passivation coating of cerium oxide (CeO_2) material is applied over the YBCO SRRs. A single photoresist mask was used in the photolithography process of patterning each SRR unit cell. A photograph of a unit cell, with the labeled dimensions, is shown in Fig. 1.

The waveguide environment was chosen for measurements because the waveguide components can easily be confined

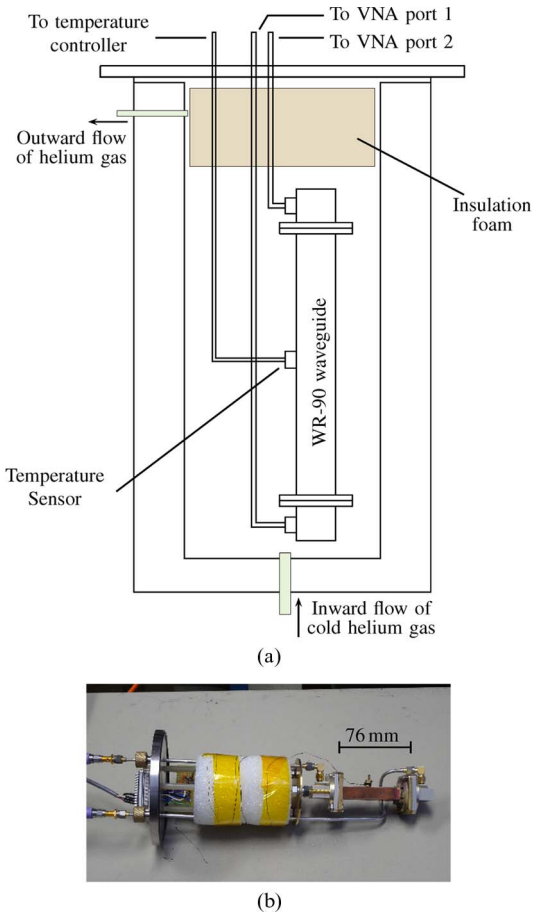

Fig. 2. (a) Sketch of the cryostat with waveguide components. (b) Photograph of the waveguide setup that fits inside the cryostat.

into a cryogenic enclosure and thus can easily be temperature controlled and calibrated. A vacuum sealed cylindrical cryostat is used to confine and cool the waveguide components, which include two aluminum waveguide to coaxial adapters and a 76.2 mm copper waveguide section for holding the HTS SRRs, Fig. 2. The inner diameter of the cryostat is 74 mm and wide enough to hold the waveguide components. Two feedthroughs in the top metal lid allow the rigid copper coaxial cables to connect to a vector network analyzer (VNA). The temperature of the copper waveguide is monitored with an attached temperature sensor. Fig. 2(a) is a sketch that shows the placement of the various components inside the cryostat along with the gas flow directions. In the measurement presented here, a setup with liquid helium is used to investigate a wider range of temperature. Fig. 2(b) shows a photograph of the waveguide unit that is placed in the flow-type cryostat. The temperature of the waveguide components is regulated by a LakeShore 330 autotuning temperature controller and TRW flow control unit. With this setup, we studied the HTS SRR in the temperature range from room temperature to 40 K.

An Agilent 8722ES VNA was used for the measurements, with the test input power level set to -10 dBm (0.1 mW). The VNA was calibrated to the end of the waveguide adapters with the Thru-Reflect-Line (TRL) method at room temperature, where the reflect standard is a short. The phase error incurred

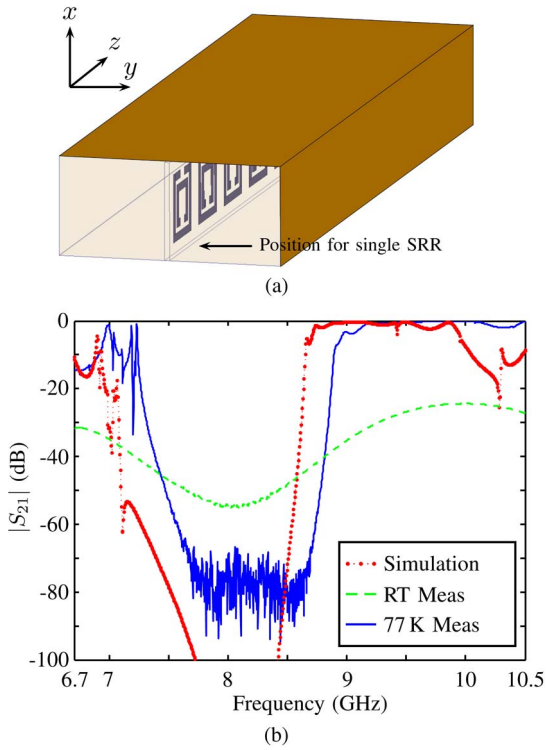

Fig. 3. (a) Placement of the HTS SRR array inside a WR-90 waveguide. The single element is placed in the same way. (b) Measured and simulated transmission (S_{21}) coefficients of an array of seven HTS SRRs placed inside a WR-90 waveguide. The measurements were taken at 77 K (solid blue) and at room temperature (dashed green).

by twisting the coaxial cable in Fig. 2(b) is removed through the calibration.

Note that the TE_{10} dominant mode excites an electric field along the sides of the square and produces an electric resonance, as explained in [9], [10]. Because of the metal wall boundary conditions, the single SRR and its images form an infinite array.

III. Measured Results

An array of seven SRRs, placed inside a WR-90 waveguide with orientation shown in Fig. 3(a), was simulated in Ansoft HFSS, a full wave finite element method (FEM) solver. In the simulation, the superconductor is modeled with a conductivity of 10^{10} S/m and the MgO substrate with a relative permittivity of 9.7 with a loss tangent of 10^{-6}. The dominant TE_{10} mode was excited in the waveguide, which has an electric field in the x direction (Fig. 3(a)), with a maximum in the middle and zero on the side walls. The simulated magnitude of the transmission coefficient ($|S_{21}|$) is plotted in Fig. 3(b) and shows a pronounced wide stop band centered around 8 GHz. Seven fabricated HTS SRRs were then placed inside a copper waveguide and measured with a VNA. The measured $|S_{21}|$ at 77 K, plotted together with the simulated result in Fig. 3(b), also shows a wide stop band. A room temperature measurement was also taken, shown as the dash curve in Fig.3 (b).

To study the temperature dependence behavior of the HTS SRR, a single element was placed inside the waveguide and the scattering coefficients were measured as the temperature was varied. At temperature below T_c, the measured transmission

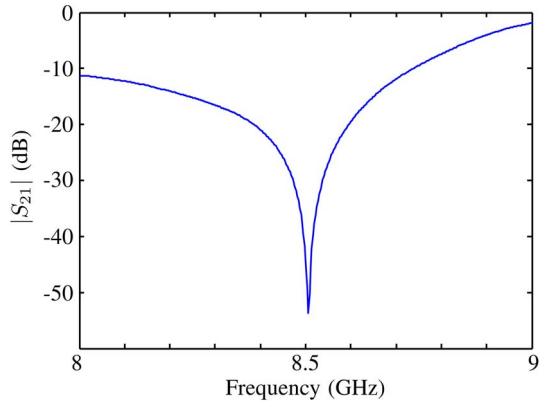

Fig. 4. Measurement of the transmission resonance (S_{21}) at 85 K.

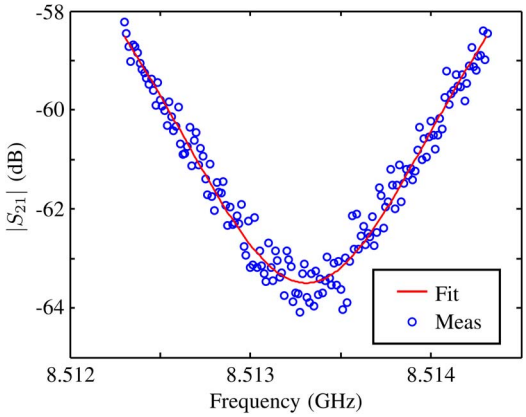

Fig. 5. Circled points show the measured transmission resonance at 81 K. The solid line is the Lorentzian curve fitted to the data.

resonances are sharp, as seen in Fig. 4. Due to the limitation of the measurement instrument, it is not possible to fully characterize the exact resonance frequency, minimum $|S_{21}|$, and 3-dB bandwidth directly for each resonance curve. We performed curve fitting to a Lorentzian distribution

$$y(f) = A - \frac{1}{2\pi}\frac{B + C(f - f_0)}{(f - f_0)^2 + D^2} \tag{1}$$

where A, B, C, D, and f_0 are the fitting parameters. The term with a C multiple is included to account for the asymmetry of the resonance curves. Fig. 5 shows the measured $|S_{21}|$ data and the fitted data around the 8.513 GHz resonance at 81 K.

The fitting process was applied to the measured transmission coefficients in the neighborhood of the resonance to give us an expression for the curve, from which the resonance frequency, minimum of $|S_{21}|$, and 3-dB bandwidth can be obtained. The associated Q-factor is defined as $f_r/\Delta f_{3\mathrm{dB}}$, where f_r is the resonance frequency and $\Delta f_{3\mathrm{dB}}$ is the 3-dB bandwidth. Thus, in Fig. 5, the fitted result (solid curve) gives $f_r = 8.5133$ GHz, $\Delta f_{3\mathrm{dB}} = 1.36665$ MHz, and $Q = 6230$. The process is repeated for measurements at other temperatures. The plot of Q as a function of temperature is shown in Fig. 6. At 87 K, we observed a peak in Q of around 42 000, which has to be estimated from the measured data. This spike in the quality factor is not expected. Further experiments are being carried out to explain this unusual frequency response observed on several

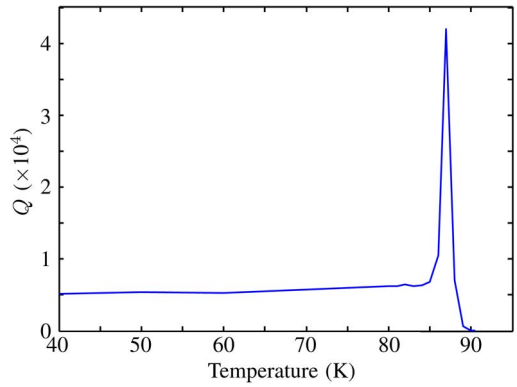

Fig. 6. Quality factor versus temperature (K) for the measured HTS SRR inside a WR-90 waveguide. It peaks around 42 000 at 87 K and saturates around 5200.

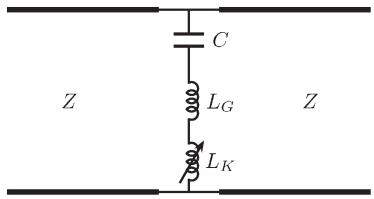

Fig. 7. Equivalent circuit model of the SRR, where the kinetic inductance L_K is temperature dependence.

samples. For comparison, a copper SRR on a Rogers TMM10i substrate was fabricated and measured at room temperature. This normal conducting SRR has $Q = 220$, which is much lower than that of the HTS SRR when $T < T_c$. It should be mentioned that we are studying the electric resonance rather than the magnetic resonance, which is located at around 3 GHz. Since this is below our waveguide cutoff frequency, we machined a planar probe setup for this measurement.

IV. Temperature Dependent f_r

The resonance frequency, f_r, of a high temperature superconducting YBCO SRR is dependent on both the ring geometry and temperature when the SRR is cooled below the critical temperature of the superconductor. The split-ring resonator can be modeled by an equivalent LC circuit model, Fig. 7, where $f_r = 1/2\pi\sqrt{LC} = 1/2\pi\sqrt{(L_G + L_K)C}$.

The inductance of a superconducting SRR can be broken down to a geometric inductance (L_G) and a kinetic inductance (L_K). The geometric inductance is the conventional inductance of the SRR structure and is temperature independent. Its value can be estimated using the expression from Saha *et al.* [19]

$$L_G = 0.000508 l_{av}\left[2.303\log_{10}\left(\frac{4l_{av}}{w}\right) - 2.853\right](\mu\mathrm{H}) \tag{2}$$

where, using the dimensions in Fig. 1, $l_{av} = 4(b - 2w - e) - g$ is the average length of the strip in mm. We can approximate the SRR with a simple single ring structure that has an effective radius r_m and the same L_G. The inductance of this simplified structure is approximated by [20] as

$$L_G = \frac{12.5\pi r_m}{8 + 11\frac{w}{r_m}} \times 10^{-6} = \gamma\mu_0 r_m \tag{3}$$

where the effective radius of the ring, r_m, and line width, w, are in meters, and γ is the transform multiplier. Equation (2) was used to solve for γ and r_m.

The kinetic inductance can be understood by equating the magnetic energy stored in an equivalent inductor, $L_K I^2/2$, to the kinetic energy of the Cooper pairs in a superconductor [21]. The kinetic inductance is a function of the London penetration depth, which depends on temperature, and can be approximated as [22]

$$L_K \approx \mu_0 \frac{l}{w} \lambda \coth \frac{t}{\lambda} = \frac{\mu_0 2\pi r_l}{w} \lambda \coth \frac{t}{\lambda} \tag{4}$$

where t is the thickness of the superconducting film, l is the length of the strip, and λ is the temperature dependent penetration depth, $\lambda(T) = \lambda(0)/\sqrt{1-(T/T_c)^2}$. Brorson *et al.* [23] estimated the absolute penetration depth $\lambda(0) = 148$ nm and Shi *et al.* [24] found $\lambda(0) = 198$ nm for $YBa_2Cu_3O_7$. The value of $\lambda(0)$ depends on the quality and structure of the material and typically lie in the range of 200–400 nm for practical materials. It will be one of the fitting parameters in fitting a theoretical model of the temperature dependence resonance frequency to the measurements.

By assuming the simple LC model in Fig. 7 for the split-ring resonator, the resonance frequency is given by

$$\begin{aligned} f_r &= \frac{1}{2\pi} \frac{1}{\sqrt{(L_G + L_K)C}} \\ &\approx f_G \left\{ 1 + \frac{2\pi r_l \lambda(0)}{\gamma r_m w \sqrt{1-\left(\frac{T}{T_c}\right)^2}} \right. \\ &\qquad \left. \cdot \coth \left[\frac{t\sqrt{1-\left(\frac{T}{T_c}\right)^2}}{\lambda(0)} \right] \right\}^{-1/2} \end{aligned} \tag{5}$$

where f_G is the resonance frequency associated with just the geometric inductance of the SRR. The critical temperature is generally known for the superconductor, but will become a parameter in the fitting process. The absolute penetration depth, $\lambda(0)$, is a second parameter. The resonance frequency f_G is not known exactly and is the third parameter. It should be close to the measured low temperature resonance frequency. This three-parameter function is fitted to the measured data through a nonlinear least square method.

The measured resonance frequency as a function of the temperature for the SRR structure is shown in Fig. 8 as the red circles. As the temperature drops, the resonance frequency increases until it saturates. The main contribution to this effect is the kinetic inductance of the superconductor, which decreases with temperature. The fitting is applied to the measured data and the result is shown as the blue dashed line in Fig. 8. From the fitted parameters, we can infer the following:

- $T_c = 91.3$ K. Above this temperature, the transmission resonances are not clearly defined. This value is close to the observed value.
- $f_G = 8.53$ GHz. This is the resonance frequency with the absence of the kinetic inductance.

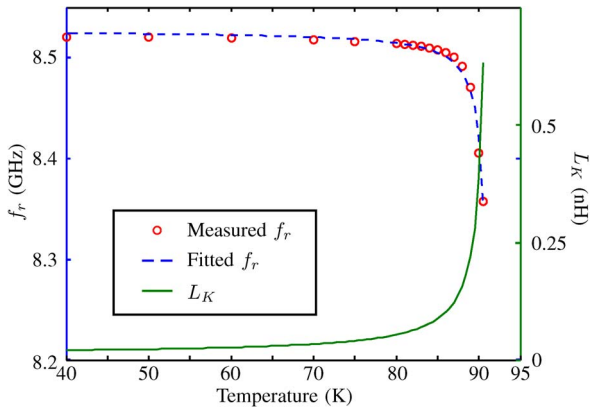

Fig. 8. Resonance frequency versus temperature. The red circle line and blue dashed line represent measured and fitted resonance frequency, respectively. The green solid line is the calculated kinetic inductance extracted from the fitting process.

- $\lambda(0) = 363$ nm. This is higher than published values of 148 nm [23] and 198 nm [24]. The slight damage of the YBCO film from the photolithography process can contribute to this higher value.

Finally, the kinetic inductance versus temperature is shown as the solid green line in Fig. 8. It shows the expected behavior, that L_K increases with temperature. This also means the total inductance $(L_G + L_K)$ increases and thus lowers the resonance frequency. The kinetic inductance of this structure is very sensitive close to the T_c, and might be used for photon detectors [25].

V. Effective Constitutive Parameter Extraction

Split-ring resonators have been shown to exhibit magnetic resonances accompanied by a negative real permeability. As mentioned earlier, they can also have electric resonances with a negative real permittivity. Let us assume that our SRR inside the waveguide can be considered an isotropic and homogeneous material. By using the parameter extraction discussed by Weir [26], the permittivity (ϵ) and permeability (μ) are retrieved, shown in Fig. 9. In the neighborhood of the resonance, discussed in Section III, Re$[\epsilon]$ is negative, which says that these are electric resonances. In addition, although not easily discernible from Fig. 9, the imaginary parts of μ and ϵ approach zero closer to the resonance as the temperature is lowered. The magnitudes of the imaginary μ and ϵ are also much smaller than those extracted from the room temperature copper SRR on TMM10i measurements.

VI. Conclusion

An array of seven YBCO on MgO split ring resonators was simulated and measured inside a WR-90 waveguide showing a pronounced wide stop band centered around 8 GHz. Furthermore, a single element ring was measured for studying the resonance frequency and quality factor versus temperature. By fitting the behavior of the resonance frequency to an expression that relates it to the penetration depth, kinetic inductance, and critical temperature, we can infer their values. The fitted T_c of 91.3 K and f_r of 8.53 GHz are close to the observed values. The inferred $\lambda(0)$ of 363 nm is higher than the values given by Brorson and Shi. This can be attributed to the slight damaging

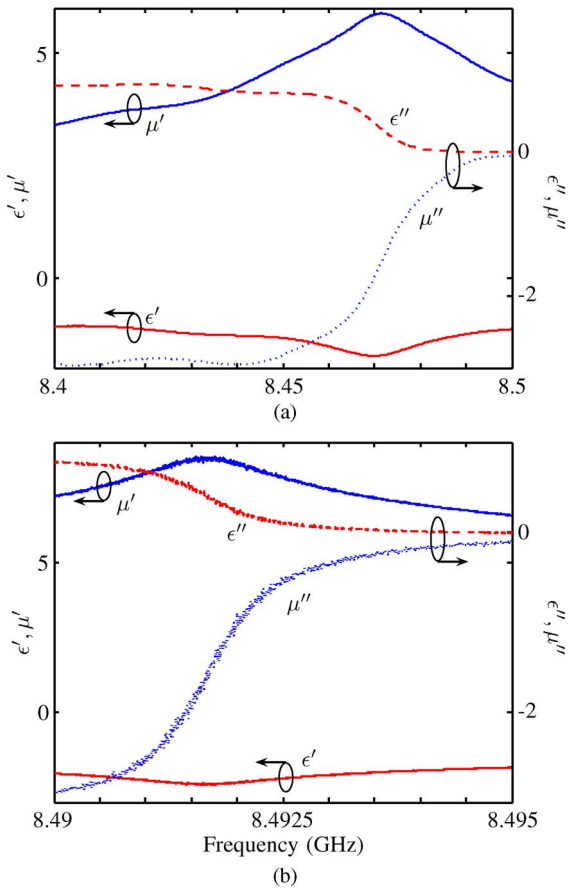

Fig. 9. Extracted relative permittivity and permeability at (a) 89 K and (b) 88 K.

of the YBCO film during the photolithography process. The kinetic inductance was shown to saturate at low temperature and vary greatly close to the T_c. The quality factor, saturating at $>$ 5000, of these HTS SRRs was shown to be much higher than the normal conductor samples. A peak of $Q \approx 42\,000$ was observed around 87 K. Finally, we have shown that these HTS SRRs have electric resonances and exhibit a negative permittivity in the neighborhood of the resonance.

ACKNOWLEDGMENT

The authors thank Dr. S. Benz at NIST for the help and discussions. Also, the authors thank Dr. A. Andrevski and F. Roesthuis for their assistance in the fabrication of the HTS SRRs.

REFERENCES

[1] J. Pendry, A. Holden, D. Robbins, and W. Stewart, "Magnetism from conductors and enhanced nonlinear phenomena," *IEEE Trans. Microw. Theory Tech.*, vol. 47, pp. 2075–2084, 1999.

[2] R. A. Shelby, D. R. Smith, and S. Schultz, "Experimental verification of a negative index of refraction," *Science*, vol. 292, pp. 77–79, 2001.

[3] L. Ran, J. Huangfu, H. Chen, X. Zhang, K. Cheng, T. M. Grzegorczyk, and J. A. Kong, "Experimental study on several left-handed metamaterials," *Progress Electromagn. Res.*, vol. 51, pp. 249–279, 2005.

[4] D. R. Smith, D. C. Vier, T. Koschny, and C. M. Soukoulis, "Electromagnetic parameter retrieval from inhomogeneous metamaterials," *Phys. Rev. E*, vol. 71, p. 036617, Mar. 2005.

[5] X. Chen, T. M. Grzegorczyk, B.-I. Wu, J. Pacheco, and J. A. Kong, "Robust method to retrieve the constitutive effective parameters of metamaterials," *Phys. Rev. E*, vol. 70, p. 016608, Jul. 2004.

[6] D. Schurig, J. J. Mock, B. J. Justice, S. A. Cummer, J. B. Pendry, A. F. Starr, and D. R. Smith, "Metamaterial electromagnetic cloak at microwave frequencies," *Science*, vol. 314, pp. 977–980, 2006.

[7] S. A. Cummer, B.-I. Popa, D. Schurig, D. R. Smith, and J. Pendry, "Full-wave simulations of electromagnetic cloaking structures," *Phys. Rev. E*, vol. 74, no. 3, p. 036621, Sep. 2006.

[8] M. Gil, J. Bonache, and F. Martıacute;n, "Metamaterial filters: A review," *Metamaterials*, vol. 2, no. 4, pp. 186–197, 2008.

[9] S. Linden, C. Enkrich, M. Wegener, J. Zhou, T. Koschny, and C. M. Soukoulis, "Magnetic response of metamaterials at 100 terahertz," *Science*, vol. 306, no. 5700, pp. 1351–1353, 2004.

[10] T. Koschny, M. Kafesaki, E. N. Economou, and C. M. Soukoulis, "Effective medium theory of left-handed materials," *Phys. Rev. Lett.*, vol. 93, p. 107402, Sep. 2004.

[11] M. Ricci, N. Orloff, and S. M. Anlage, "Superconducting metamaterials," *Appl. Phys. Lett.*, vol. 87, no. 3, p. 034102, 2005.

[12] M. C. Ricci and S. M. Anlage, "Single superconducting split-ring resonator electrodynamics," *Appl. Phys. Lett.*, vol. 88, no. 26, p. 264102, 2006.

[13] M. Ricci, H. Xu, R. Prozorov, A. Zhuravel, A. Ustinov, and S. Anlage, "Tunability of superconducting metamaterials," *IEEE Trans. Appl. Supercond.*, vol. 17, no. 2, pp. 918–921, Jun. 2007.

[14] H.-T. Chen, H. Yang, R. Singh, J. F. O'Hara, A. K. Azad, S. A. Trugman, Q. X. Jia, and A. J. Taylor, "Tuning the resonance in high-temperature superconducting terahertz metamaterials," *Phys. Rev. Lett.*, vol. 105, p. 247402, Dec. 2010.

[15] J. G. Bednorz and K. A. Müller, "Possible high T_c superconductivity in the BaLaCuO system," *Zeitschrift fr Physik B Condensed Matter*, vol. 64, pp. 189–193, 1986, 10.1007/BF01303701.

[16] M. K. Wu, J. R. Ashburn, C. J. Torng, P. H. Hor, R. L. Meng, L. Gao, Z. J. Huang, Y. Q. Wang, and C. W. Chu, "Superconductivity at 93 K in a new mixed-phase Y-Ba-Cu-O compound system at ambient pressure," *Phys. Rev. Lett.*, vol. 58, pp. 908–910, Mar. 1987.

[17] MgO magnesium oxide single crystal substrates-SPI supplies. [Online]. Available: http://www.2spi.com

[18] J. Mazierska, D. Ledenyov, M. V. Jacob, and J. Krupka, "Precise microwave characterization of MgO substrates for HTS circuits with superconducting post dielectric resonator," *Supercond. Sci. Technol.*, vol. 18, no. 1, p. 18, 2005.

[19] C. Saha and J. Y. Siddiqui, "A comparative analyis for split ring resonators of different geometrical shapes," in *Proc. IEEE Appl. Electromagn. Conf. (AEMC)*, Dec. 2011, pp. 1–4.

[20] T. K. Ishii, *Handbook of Microwave Technology*. New York: Academic Press, 1995.

[21] T. Van Duzer and C. W. Turner, *Principles of Superconductive Devices and Circuits*. New York: Elsevier, 1981.

[22] W. Henkels and C. Kircher, "Penetration depth measurements on type II superconducting films," *IEEE Trans. Magn.*, vol. MAG-13, no. 1, pp. 63–66, Jan. 1977.

[23] S. D. Brorson, R. Buhleier, J. O. White, I. E. Trofimov, H.-U. Habermeier, and J. Kuhl, "Kinetic inductance and penetration depth of thin superconducting films measured by THz-pulse spectroscopy," *Phys. Rev. B*, vol. 49, pp. 6185–6187, Mar. 1994.

[24] L.-B. Shi, Y.-F. Wang, Y.-Y. Ke, G.-H. Zhang, S. Luo, X.-Q. Zhang, C.-G. Li, H. Li, and Y.-S. He, "A study on the microwave responses of YBCO and TBCCO thin films by coplanar resonator technique," *Chin. Phys.*, no. 10, pp. 3036–3041, Oct. 2007.

[25] G. Vardulakis, S. Withington, D. J. Goldie, and D. M. Glowacka, "Superconducting kinetic inductance detectors for astrophysics," *Meas. Sci. Technol.*, vol. 19, no. 1, p. 015509, 2008.

[26] W. Weir, "Automatic measurement of complex dielectric constant and permeability at microwave frequencies," in *Proc. IEEE*, Jan. 1974, vol. 62, no. 1, pp. 33–36.